4

Numerical Simulation of Abrasion of Particles

Manoj Khanal[1] and Rob Morrison[2]
[1]*Queensland Centre for Advanced Technologies, Earth Science and Resource Engineering, Commonwealth Scientific and Industrial Research Organization, Technology Court, Pullenvale,*
[2]*Julius Kruttschnitt Mineral Research Centre, University of Queensland, Indooroopilly, Australia*

1. Introduction

Abrasion is a surface breakage event where irregular surfaces of particles are removed. It produces smoothed surfaces/particles by comminuting irregular edges. Depending on the application, abrasion can be a desired or undesired process, and may happen either naturally or intentionally. For example, in some industries where spherical particles are end products, abrasion can be a desired process but in some process industries it is undesired because it produces dust, which makes it difficult for handling, as well as increasing the potential for losses of material. In some cases, natural phenomena (weathering, time dependent effect, age, and contact) can abrade materials and sometimes abrasion of materials is enhanced by applying energy. The loss of surface layers of particles due to weathering can be considered as a natural abrasion process whereas the use of mills to generate fines are considered as abrasion via applied energy.

Continuous abrasion of materials also implies particle size reduction. When a particle is stressed, the particle response depends on its size and shape, and the conditions under which stress is applied. In general, the governing parameters for abrasion can be differentiated into three groups – material parameters, process parameters and machine parameters. The initial stress condition (history), diameter (scale), shape and size, homogeneity and type of materials are known as material parameters. The process parameters include type of stress, particle-particle configuration, stressing velocity and frequency, temperature, specific energy. Similarly, the machine parameters cover shape, size and hardness of the stressing tool, and size and geometry of the stressing machine. The requirement (shape and size) of the final abraded products depends on the better selection of these parameters.

The diversity and the purpose of tasks to be performed during abrasion have led to the development of a range of abrasion testing machines. There is no uniform criterion available for classifying abrasion and the system used for naming machines is not standardized. Hence, a particular type of machine may have several names. Similarly there is no any

standard definition of mechanisms of size reduction ratio. Mostly it is considered as a slow process where a "significantly less" amount of materials are removed from the parent material. There is no definition of "significantly less" which classifies the process as abrasion. For example, if a parent particle loses 10% of its mass during fracture process then it is termed as comminution, if the outputs are lumps larger than a few centimetres then the process is defined as crushing and if the outputs are in finer and in millimetre ranges the process is called milling (Rumpf, 1995). A similar definition of abrasion is not available in the literature. In short the definition of abrasion is more of a concept rather than a mathematical definition.

There are various methods and machines, however in mineral processing tumbling mills are typically used, to study the abrasion. This paper is also based on the tumbling mill. A tumbling mill can be operated in a controlled environment, where basically, three different stages of particle failure can be observed. The first stage is surface failure where particles lose their edges and surfaces to become more rounded shapes. Surface breakage mechanisms like "abrasion" and "attrition" can be classified within this stage.

Surface breakage is followed by the second stage which involves body breakage of particles. In this stage, parent particles lose a large fraction of their mass and generate progeny. This can be termed as body breakage or, most commonly, comminution. The third stage can be termed as secondary breakage, where already comminuted particles disintegrate further. The fragments generated in the second stage further generate sub-fragments. These three stages depend upon the tumbling time and the intensity of stresses generated in the particles.

In milling, particles of interest are processed to produce surface breakage events. Secondary media like steel balls and/or pebble ports maybe used to modify the product size distribution. As the mill rotates for abrasion milling, primary media (rock particles), and secondary media (grinding balls) if present, tumble against each other and the material breaks mainly by abrasion. Extensive experimental work has been done by Loveday and Naidoo (1997), Loveday et al. (2006), Loveday and Dong (2000), Loveday and Whiten (2002) to study the abrasion of mineral particles. Most of these studies are empirical in nature. A few studies (Morrison and Cleary, 2004, Khanal and Morrison, 2008), have used the discrete element method (DEM) to study the abrasion behaviour of particles. There is no globally accepted model which describes the abrasion of particles in general.

The objective of this paper is to study the relevance of 3D Discrete Element Modelling (DEM) simulation of abrasion in small scale tumbling mills. The paper also focuses on DEM simulation to investigate ore abrasion resistance and evaluation of abrasion process parameters of spherical and non-spherical particles in a milling environment. Different mill sizes are selected for this study. Various process parameters, for example, effect of particle size, milling time and stiffness of particles on abrasion characteristics have been evaluated. The paper also discusses effect of surface roughness on the particle trajectories, collision force, collision energy, and energy spectra. These DEM results are compared with experimental results where applicable.

As the paper deals with the abrasion of particles, we wish to avoid body breakage. The grinding time for the abrasion process has been noted from the experiments (Banini, 2000) and it represents an abrasion only case, hence the descriptions are based on it. The DEM

simulations have been carried out in order to support and analyse experimental interpretation with numerical simulations.

2. Experimental work

Experimental data were extracted from Banini (2000). Four different mill sizes of 0.2 m, 0.3 m, 0.6 m and 1.1 m internal diameter were manufactured. Each mill has rectangular lifters of 30 mm in height placed at regular intervals. The number of lifters was different in different mills. Table 1 shows the number of lifters present and the rotational speed of each mill. The rotational speeds for 1.1 m and 0.6 m diameter mills were 60% and for 0.3 m and 0.2 m mills were 70% of the critical speed. During each revolution, particles are lifted to a maximum point and then released under gravity. However the particles may reach their highest point after leaving contact with the lifter.

Mill Diameter	**1.1 m**	**0.6 m**	**0.3 m**	**0.2 m**
Mill Speed (rad/sec)	2.53	3.42	5.66	6.93
Number of Lifters	12	8	6	4
Size Fraction (mm)	**Release Heights (m)**			
90.0 – 75.0	0.94	0.46	0.24	0.13
63.0 – 53.0	0.97	0.52	0.24	0.14
45.0 – 37.5	0.97	0.53	0.27	0.14
31.5 – 26.5	0.97	0.54	0.27	0.16

Table 1. Size fraction, mill speed, mill diameter, release height and number of lifters used in experiments (Banini, 2000)

There are centrifugal and frictional forces when the particles are in contact with the liners and lifters. The falling of particles from the highest point will transfer maximum amount of energy to the particles during each revolution with a minimum level of projection/ trajectory (Banini, 2000). Table 1 also shows the maximum release heights for different mills and size fractions. For the largest particles (considered here) in the 1.1 m mill, 0.94 is the release height observed from the experiments, which is 85% of the height of the mill. Similarly, for 0.6 m, 0.3 m and 0.2 m mills, the release heights are 76%, 80% and 65%, respectively of the mill diameter. This increases with the decrease in size of the particles in the mill. This is due to the fact that the center of mass of particles lie closer to the mill shell and this provides relatively more stability to the smaller particles, hence they are lifted higher than the larger particles.

Several rock types were tested. The details of the rock types can be found in (Banini, 2000). Table 2 shows the number of particles tested per size fraction in each mill. Extended tumbling generates body breakage and produces large fragments. Particles which have been repeatedly impacted during the tumbling process generate incremental (progressive) damage, and subsequently break (body breakage) at low stressing energies. This was confirmed by Banini (2000), as tumbling time increased beyond 10 min the original particles began to undergo body breakage for the considered cases. Further, Loveday and Naidoo

(1997) have mentioned that particle size reduction results from grains loosened by multiple impacts rather than from rubbing of surfaces.

Size Fraction (mm)	Number of Particles
90.0 – 75.0	8
63.0 – 53.0	12
45.0 – 37.5	20
31.5 – 26.5	36

Table 2. Number of particles tested per size fraction in each mill (Banini, 2000)

Increasing the mill load leads to an increase in wear rate of particles (Loveday and Naidoo, 1997). It has been observed that the rock–rock collision and overcrowding at the toe of the mill results in production of unusually fine material (Banini, 2000). The rate of abrasion of rocks can be reduced by the presence of fines and/or chips (Loveday and Dong, 2000). Table 3 shows the number of rocks per charge for each mill and size fraction, respectively to reduce the rock–rock collision.

Size Fraction (mm)	Mill diameter (m)			
	1.1	0.6	0.3	0.2
90.0 – 75.0	4	4	2	2
63.0 – 53.0	6	6	3	2
45.0 – 37.5	10	10	4	2
31.5 – 26.5	18	18	6	4

Table 3. Maximum number of particles in each mill and size fraction to abrasion only case for rock–rock collisions (Banini, 2000)

3. Numerical simulations

In DEM, particles are considered to be distinct elements. The laws of motion and material constitutive laws are applied to each element. In this paper, DEM simulations were carried out with a commercially available package (EDEM, 2006). The Hertz–Mindlin (no slip) contact law has been used to model the contact interaction among entities. The milling condition and parameters used in the experimental work were simulated. The mills and lifters were designed in SolidWorks (2006) and imported into EDEM. The required number of particles for each simulation was generated by varying size and distribution of the sample particle. Tables 4a and 4b show the material properties assigned to particles and mills, and number and size of particles used for the simulations in different mills, respectively.

	Poissions ratio	Shear Modulus (GPa)	Density (kg/m^3)
Particle	0.25	0.1	2650
Mill	0.29	80	7861

Table 4a. Particle and mill properties for simulations

Loveday and Naidoo (1997) found that the abrasion rate per unit mass increases significantly with rock mass. In abrasion modeling it is difficult to relate experimental work to DEM simulation results. Therefore, different hypotheses and assumptions have to be made to the data available from the simulations to compare with experimental results. Generally, it was assumed that the number of collisions in the simulations is responsible for particle disintegration (abrasion) and each collision accounts for an incremental damage and certain amount of mass is comminuted from the parent specimen. In other words, the number of collisions (with suitable assumptions and relations) can be compared with experimental mass losses from the particles. A good correlation has been found between measured particle mass loss and the DEM estimate of cumulative frictional energy absorbed by the particles (Cleary and Morrison, 2004).

Simulation	Mill size (m)	Number of particles	Particle size distribution (random distribution, mm)
1	1.1	8	72 - 90
2		12	53 - 63
3		20	37.5 - 45
4		36	26.5 - 31.5
5		38	26.5 - 90
6		76	26.5 - 90
7	0.6	4	75 - 90
8		6	75 - 90
9		8	75 - 90
10		10	37.5 - 45
11		12	53 - 63
12		18	26.5 - 31.5
13		20	37.5 - 45
14		36	26.5 - 31.5
15		38	26.5 - 90
16	0.3	8	26.5 - 90
17		15	72 - 90
18	0.2	10	26.5 - 90

Table 4b. Numbers and sizes of particles used for simulations in different mills

The paper also deals with non-spherical particles. They were generated by combining different individual particles. The figure shown in Table 5 illustrates the complex particle which can be formed by combining many smaller particles. Rough surfaces of the template

show the asperities and roughness present on the particle. The required number of particles for each simulation was generated by varying size and distribution of the template particle. Table 5 shows the assigned particle and mill material properties.

Different particle structures have been simulated to study the effect of surface roughness in abrasion. Eight different particles with random distributions in the range of 70 to 90mm have been simulated as the load in a 1.1m mill. The roughness of particles was varied from particles having 15 ''humps'' (asperities) to perfectly spherical particles without ''hump.'' The template particle shown in Table 5 represents a particle structure with 15 humps. Table 5 shows the number of surfaces created on the template particle to simulate eight-particle systems in a 1.1m mill.

Rough surface	**Mass, kg**	**Remarks**	**Template of a particle**
Single sphere	7.57	planet	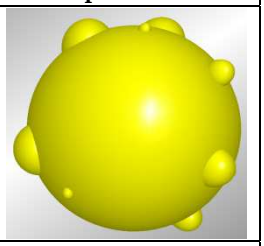
1	7.36	1_surface	
7	4.66	7_surface	
13	4.55	13_surface	
15	4.55	15_surface	
Particle and mill properties for simulations			
	Poisson's ratio	*Shear Modulus (GPa)*	*Density (kg/m³)*
Particle	0.25	0.1	2650
Mill	0.29	80	7861

Table 5. Particles having different types of rough surfaces used to simulate an 8-particle system in 1.1m mill

4. Results and discussion

4.1 Spherical particles

4.1.1 Particle trajectories

Figure 1 shows the results of DEM simulations of particle trajectories in the 1.1 m and 0.6 m mills for mills containing 8, 12, 20 and 36 particles. The figures suggest that the particles follow the circumference of the mill up to the maximum height the lifter can take. Then due to gravity, the particles fall within the mill. At the steady state condition, the lifters throw the particles as far as possible in a projectile trajectory. Depending on the population (density) of particles inside the mill, the fallen particles hit either another particle or the mill shell. For the lightly loaded conditions, the particles do not collide with each other before hitting the mill shell. But if the mill is overcrowded with particles, many inter-particle collisions will occur and finer particles will be generated. Hence, particle–particle interaction does not appear to occur until a critical number of particles and increase in mill loads increase in wear rate of the particles (Loveday and Naidoo, 1997; Banini, 2000).

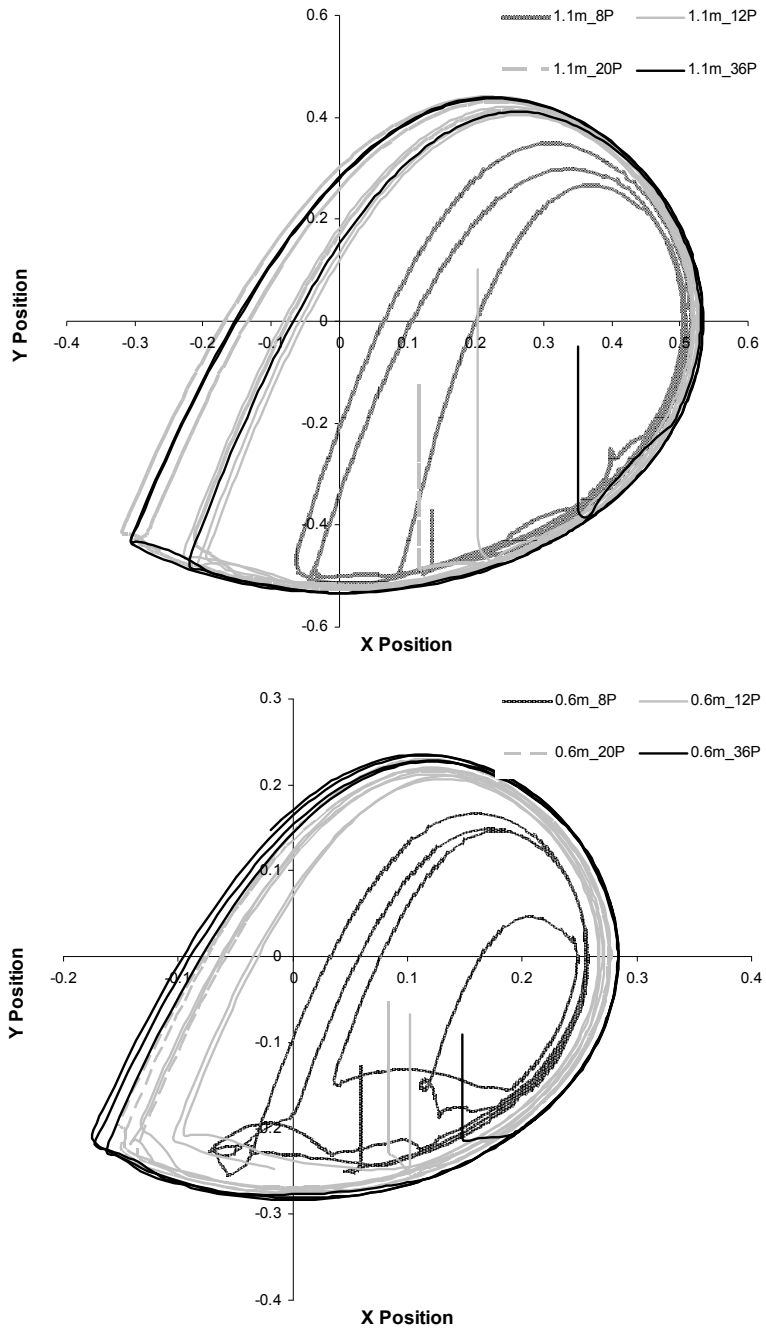

Fig. 1. Particle trajectories for 1.1 m (left) and 0.6 m (right) mills

4.1.2 Release height analysis

Particles on the lifters are lifted up to a certain height and release due to gravity. The lift-up and release heights are important as they impart potential and kinetic energy to the particles, as a result they govern the collision energy. It was noted by Djordjevic et al. (2006) that smaller particles are lifted higher than larger particles as their centres of mass are closer to the mill shell than the outer edge of the lifter bar.

The release heights were measured experimentally (Banini, 2000) by observing the motion of the charge through the perspex front cover of the mill. In the simulations, DEM allows the user to calculate the release height by tracking the simulated trajectories of the rock particle. The experimental release heights are shown in Table 1 for different mill sizes and size fractions. The maximum achievable heights of the particles in different mills during simulations are shown in Figure 2. The figure shows the height of the particles versus time for 1.1, 0.6, 0.3 and 0.2 m mills with 8, 10, 12, 15 and 36 particles. The average release height for 1.1 m mill with 36 particles is 0.94 m in simulations whereas 0.97 m is in experiments. Similarly, for 0.6 m mills, the average release height is 0.52 m in simulations and 0.54 m in experiments. The release height was calculated from the difference in position of the particles (along the height of the mill) in one revolution of the mill. The slight difference in the release height is due to the selection of particles to trace the height in experiments and simulations. The release height maybe different depending on the size of the particles selected to calculate the release height as size and shape (for the position on lifter) of the particles influence the lift-up height (Djordjevic et al., 2006).

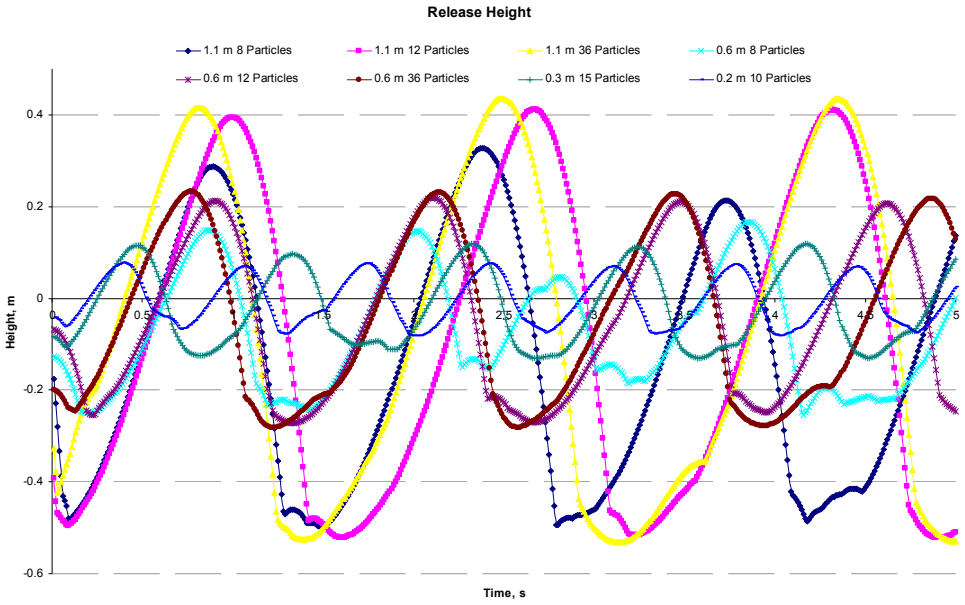

Fig. 2. Simulated release heights for different mills

4.1.3 Collision energy analysis

It is important to understand how particles accumulate and dissipate energy during abrasion. Figure 3 shows the energy gained by all particles in the 1.1 mill consisting of 20 particles for 5 s. Particles accumulate potential energy during the lift-up process. In the 1.1 m mill, particles are lifted higher than in the 0.6 m mill. Hence, particles in the 1.1 m mill gain and accumulate more energy. When the particles are released, they collide with other particles or the mill shell and transfer a portion of the accumulated energy to abrasion. The gain in the potential energy in the particles is confirmed by an inclined curve (from left to right) in Figure 3. When the particles are released from the lifters, the particles gain the velocity and the potential energy will be converted into the kinetic energy. The released particles hit other particles or the mill shell and use the kinetic energy to produce fragments (the disturbances in the vertical line). Due to the higher release height, in 1.1 m mill the particles have more available energy to release, hence, higher amount of potential energy will be imparted, thus higher kinetic energy.

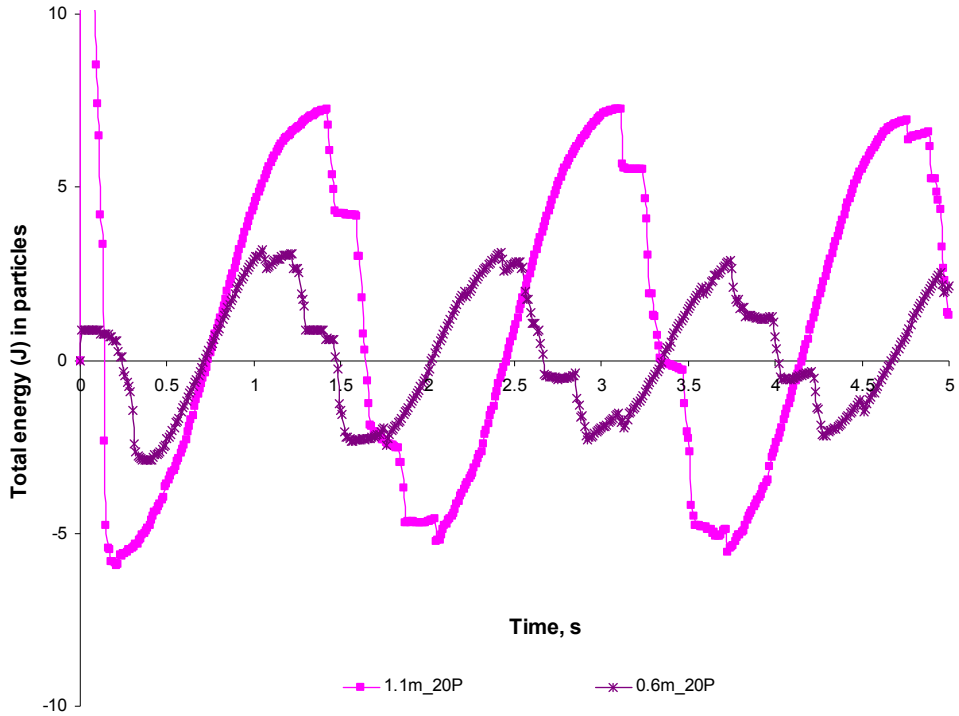

Fig. 3. Total energy gained by particles during tumbling

The same size distribution of particles in larger mills gains and dissipates higher energy than the smaller mills. However, the mill size is not the only factor which affects the gain in the energy for different size fraction of particles. The size fraction (size) of the particles and

lifter size also influence the lift-up (release) height (Djordjevic et al., 2006) and hence, the collision energy.

4.1.4 Effect of mill diameter on abrasion

Three different mills (diameter 1.1, 0.6 and 0.3 m) were simulated with same parameters and throughput (eight particles) to investigate the effect of mill diameter on abrasion of particles. The mills were running at 2.53 rad/s (60% of critical speed for 1.1m mill). The same amount, size and mass of particles in different mills causes different "filled volume" in different sized mills. In smaller mills, the particle distribution is denser than larger mills with same number and size of particles. Table 6 shows the number of collisions in the mills. In the 0.3 m mill, due to less free space inside the mill, one can expect more collisions than in the other two cases. However, it seems from the data shown in Table 6 that it is not valid for 1.1 m mills. This maybe because of the very few particles in the larger mill, where the filled volume ratio (= total volume of particles/ volume of mill) was very low. The number of collisions is almost similar in the 0.6 and 1.1 m mills. This suggests that these two mills produce almost identical outputs for eight particles.

Mill diameter, m	**0.3**	**0.6**	**1.1**
Particles – all collisions, Hz	297	247	265

Table 6. Number of collisions for different mill sizes for the same mass of eight particles

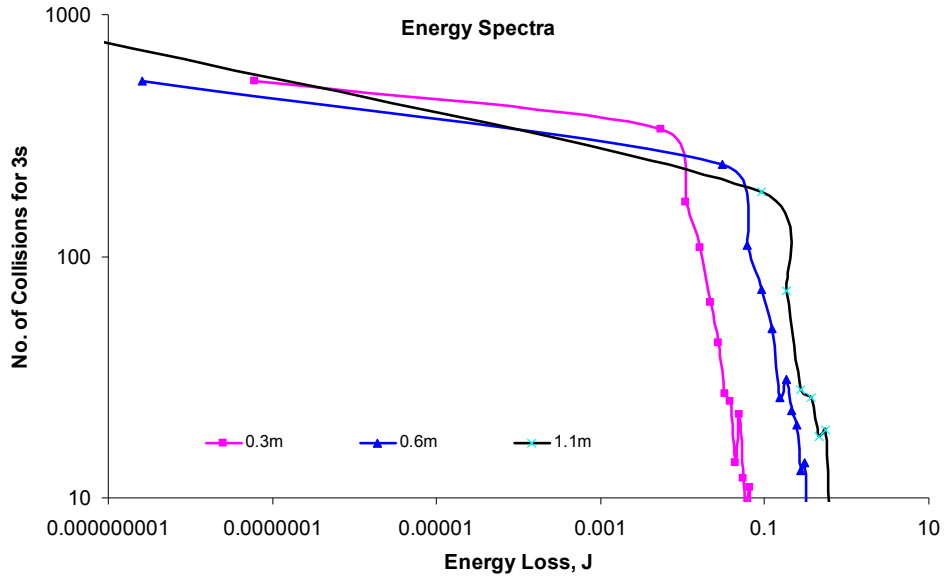

Fig. 4. Energy spectra for different mill diameters

Figure 4 shows the energy spectra for different sized mills (for the same parameters and particle loading conditions). The 0.3 m mill requires the least energy, among the three mills, to achieve the same amount of collisions. In short, the 0.3 m mill generates more collisions than the other two mills for the same expenditure of energy. Similarly, it can be observed that in the 0.3 m mill, particle–particle collisions are higher than in the other two types (Figure 5). This strengthens the hypothesis that a larger fraction of finer particles are generated in smaller mills than in the larger mills due to inter-particle collisions. The 0.3 m mill seems to be an energy efficient mill for disintegration of particles. However it generates more fragments than the others. As seen from Figure 5, the 0.6 m and 1.1 m mills have approximately same amount of inter-particle collisions with a noticeable difference in energy. For example, for 50 collisions, energy dissipated is approximately 0.15 J, 0.1 J and 1.5 J for 0.3 m, 0.6 m and 1.1 m mills, respectively. This shows, the 0.6 m mill is more energy efficient than the 1.1 m mill to achieve same number of collisions.

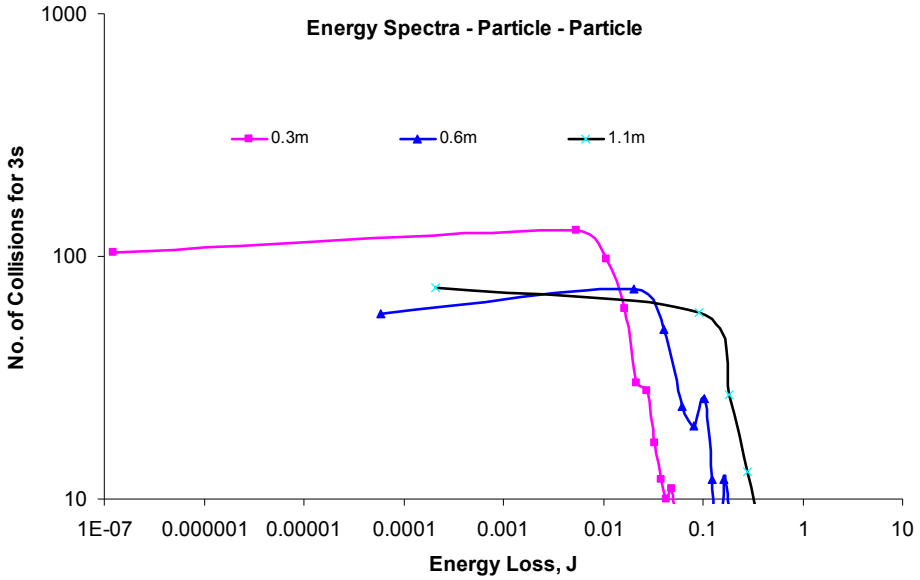

Fig. 5. Energy spectra (particle-particle) for different mill diameters

4.1.5 Effect of fraction of critical speed on tumbling

For similar diameter mills, different researchers have used different fractions of the critical speed of the mill. In this case, it is interesting to investigate the effect of critical speeds in tumbling parameters. The 1.1 m mill with 38 particles was chosen to study the effect of critical speeds in tumbling. Table 7 shows the number of collisions with respect to tumbling time at 60%, 70% and 75% of the critical speed. An increase in the tumbling speed causes a somewhat increase in the number of collisions, which is as expected. For 70% and 75% of the critical speed, there is not much difference in the number of collisions whereas at 60% and 70% of the critical speed there is noticeable increase in the number of collisions. This implies

that a 5% variation in the rotating speed may not significantly influence the results. But in the long run (more than 30 s of simulation), going to 75% of the critical speed only causes a small increase in the number of collisions. This is further confirmed by Figure 6.

Critical speed, %	**60**	**70**	**75**
Particles – all collisions, Hz	1306	1501	1501

Table 7. Number of collisions for different critical speeds of the 1.1m mill

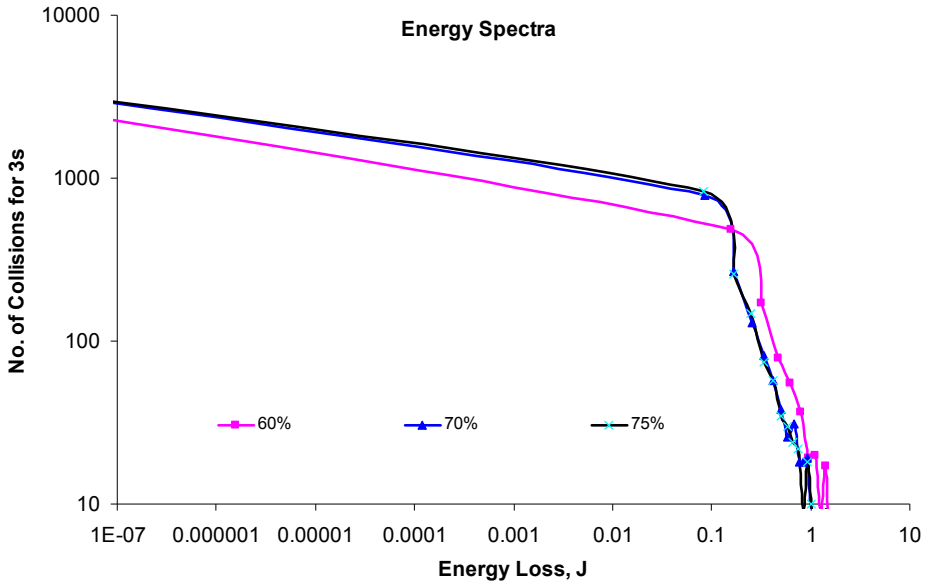

Fig. 6. Energy spectra observed for different rates and range of rotation.

Figure 6 shows the energy spectra at rates of rotation. At higher rotating speed relatively more energy is lost during particle collisions. The energy lost and the number of collisions is almost identical in the mill rotating at 70% and 75% of critical speed. However, the mill rotating at 60% of the critical speed shows relatively less collisions for almost same amount of energy loss. At lower speed (65% critical speed) the charges cannot reach the maximum height (compared to 70% and 75% critical speed), however the charges tumble effectively in the mill. This infers that the mill rotating at 70% and 75% of the critical speed will generate more fragments and is more suitable for incremental body break-age of the particles whereas lower rotating speeds are suitable for abrading the particles.

4.1.6 Effect of tumbling time

It has been observed that the effect of the tumbling time is pronounced. As the milling time increases, the cumulative number of collisions also increases. The number of collisions can

be related to the abrasion of particles. However average number of collisions remains same. In the experiment, the particle size distribution curves show the generation of more fine material as the grinding time increases. Due to a large number of collisions in the beginning of the simulation, higher energies are lost at the initial stage of the tumbling. Once the mill reaches steady state, the rate of energy losses also become uniform and reaches a steady state condition. The effect of grinding time in collisions can be verified by the energy spectra curves observed at different tumbling times.

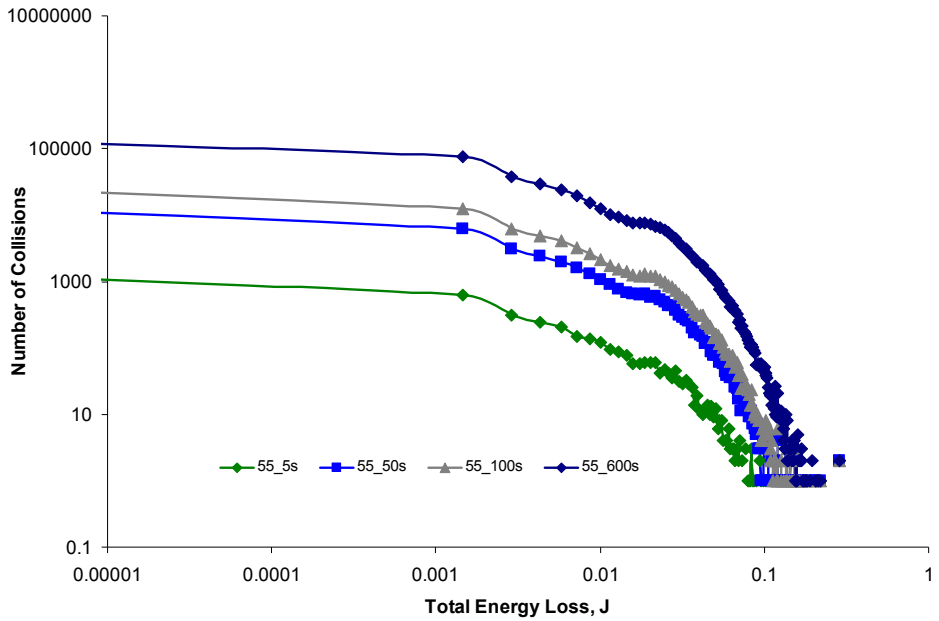

Fig. 7. Number of collisions versus total energy loss for -55.5+37.5 class particles for different grinding time (Xs_in the legend shows the milling time).

The frequency distributions of the energy losses can be determined from the individual collision events. These collision energy spectra provide an opportunity for improved understanding of the various contributions to the overall energy dissipation within the mill. Knowledge of effect of mill parameters on the energy spectra will allow in selecting useful attributes to increase the efficiency of comminution. Figure 7 shows the collision – energy loss relationship for the abrasion at different time. The energy spectra distribution in the graph shows a similar trend. At short tumbling time, few collisions occur, so less energy loss. As the grinding duration increases, the number of collisions also increases. The maximum energy dissipation is relatively larger for more tumbling time than for less tumbling time. A large number of collisions are observed at the lower energies. Based on a hypothesis – number of collisions increases the production of fragments – the 600 seconds tumbling time produces more fragments with fines than the 5 seconds tumbling time with an identical size fraction. Due to a large number of collisions in the beginning of the simulation, higher energies are lost at the initial stage of the tumbling.

4.1.7 Effect of particle size

Experimental investigations showed that the effect of particle size in abrasion is not so influential (Unpublished report). It has been reported that the changes in particle size for the same tumbling time of 600 seconds tend to produce similar curves for the smaller sizes.

In the DEM simulations, the number of particles in the mill was varied to represent different particle sizes for the same total mass. For example, 3 kg of total mass can be represented by the size classes -55+37.5, -37.5+26.5, -26.5+22.4 and -22.4+16 with 24, 72, 157 and 334 particles, respectively.

It is evident from the literature that the particle–particle collisions show different failure mechanism than the particle–wall collisions and the particle velocity also govern the severity of particle failures (Khanal et al, 2007). Table 8 shows that the fewer inter-particle collisions occur in the tumbling mill than the particle-mill shell collisions. Hence, majority of particle breakage occurs due to particle-mill shell collisions. As the number of particles increases in the mill, the number of collisions (total and inter-particle) also increases, which are shown by -22.4+16 mm size class particles. More particles show more collisions with a large number of inter-particle collisions. This demonstrates that large number of particles in a mill increases particle–particle collisions and a reasonably high amount of dust will be produced. This was observed experimentally by Banini, (2000); Loveday and Naidoo, (1997). The rock overcrowding at the toe of the mill also enhances the inter-particle collisions.

Size class (mm)	Total collisions (MHz)	Particle-particle collisions (MHz)
55-37.5	10.17	33.04
37.5-26.5	32.52	16.22
26.5-22.4	80.32	56.36
22.4-16	186.24	130.67

Table 8. Total and particle-particle collision for different size classes for 600 seconds

Figure 8 shows the relationship between number of collisions and total collision energy loss for 5 seconds. The four curves follow a similar trend in dissipating the collision energy. Large number of collisions occurs at the lower energy levels. The -55+37.5, -37.5+26.5, -26.5+22.4 size classes require more energy to achieve the same number of collisions as occurred in -22.4+16 size class. The density of the particles (population) in -22.4+16 size class is higher than in the other three classes, so, the number of collisions in former is higher than in the latter. Therefore, it can be suggested that the particle size also influences the generation of fines. Material behaviour changes from elastic to plastic as particle becomes smaller (Rumpf, 1995). It is a very difficult and high energy process to break (or abrade) the tiny particles as those particles may have very few flaws present in them compared with large particles.

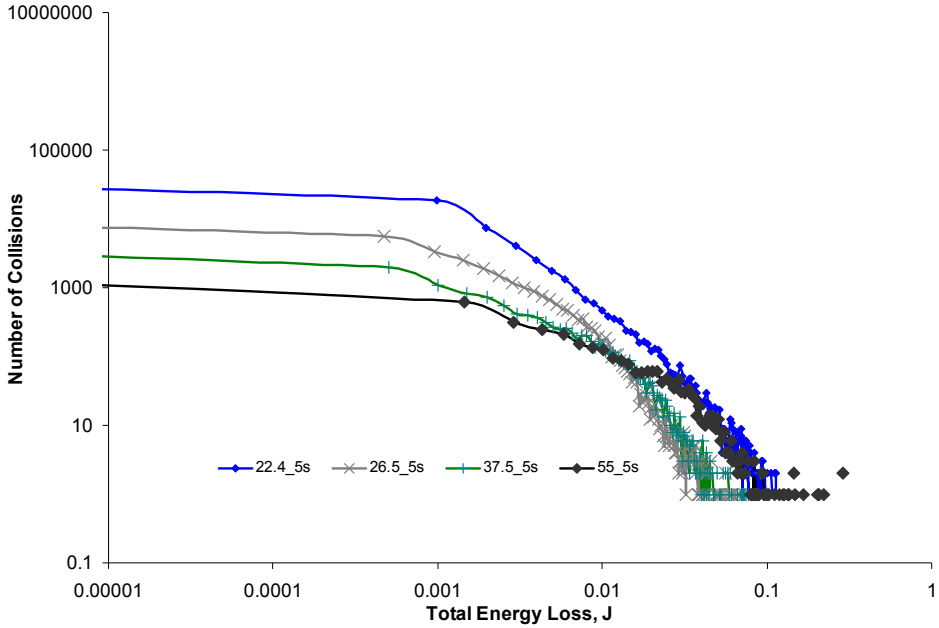

Fig. 8. Collisions versus total energy loss for different size classes after 5 seconds of mill operation.

4.1.8 Effect of particle modulus

The particle size distribution of the progeny depends upon the type of parent materials. In other words, the variation in the material properties causes the difference in progeny particle size distributions. The experimental progeny particles are related to the simulated number of collisions as, in simulations number of collisions causes the generation of daughter particles. It can be expected that the larger modulus of particles (stiff particles) generate relatively more collisions than the lower modulus of particles (soft particles).

Since the modulus is a measure of the stiffness of a given material, four different shear moduli (0.1, 1, 10 and 100 MPa) were chosen to represent different ore types ranging from very soft to moderate as hard. Each ore type is simulated for exactly the same conditions except for the change in shear modulus. Figure 9 shows the number of collisions versus total energy loss for different types of particles. The four curves follow similar trends in dissipating the collision energy. Large numbers of collisions occur at the lower energy levels. The low shear modulus particles require more energy to achieve the same number of collisions as occurred with high modulus particles. The figure shows that as the modulus of particles increases the number of collisions also increases. In other words, at the same amount of energy, the higher shear modulus of particles generates more collisions than the

lower modulus of particles. This suggests that stiff particles should be more energy efficient in generating fragments than the less stiff particles.

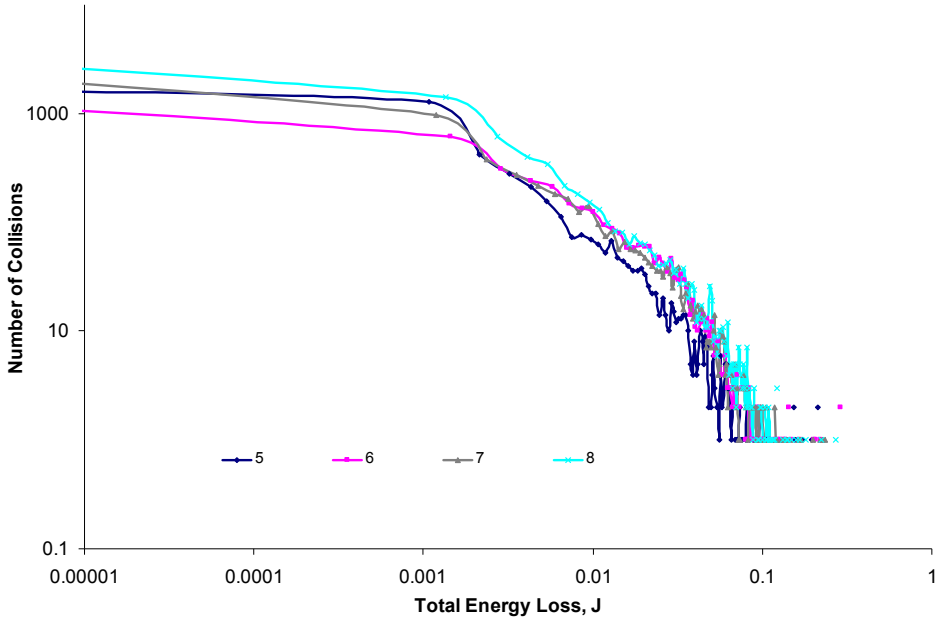

Fig. 9. Collisions versus total energy loss for different particles (5, 6, 7 and 8 represent shear modulus of 1e5, 1e6, 1e7 and 1e8 Pa respectively).

4.2 Non-spherical particles

4.2.1 Particle trajectories

Figure 10 shows the particle trajectories in a 1.1m mill for different non-spherical particles. Particles follow the circumference of the mill up to a maximum height the lifter can take them. Then, due to gravity, the particles fall randomly within the mill. However, once the mill reaches a steady-state condition, the lifters try to throw the particles as far as possible in a projectile trajectory. Depending on the population (density) of particles inside the mill, the fallen particles hit either ball or shell. For the optimum condition, the particles do not collide with each other before hitting the mill shell. But if the particles are overcrowded, notable inter-particle collisions will occur and finer particles will be generated. Hence, particle-particle interaction does not appear to occur until a critical number of particles. An increase in the mill load results in an increase in wear rate of the particles. The shorter trajectories for the same particle in the graphs are due to the data extraction at the unsteady-state condition (i.e., before 2.3 s of simulation). As the centre of mass of smaller particles is closer to the mill shell, they are lifted a little higher than the larger particles.

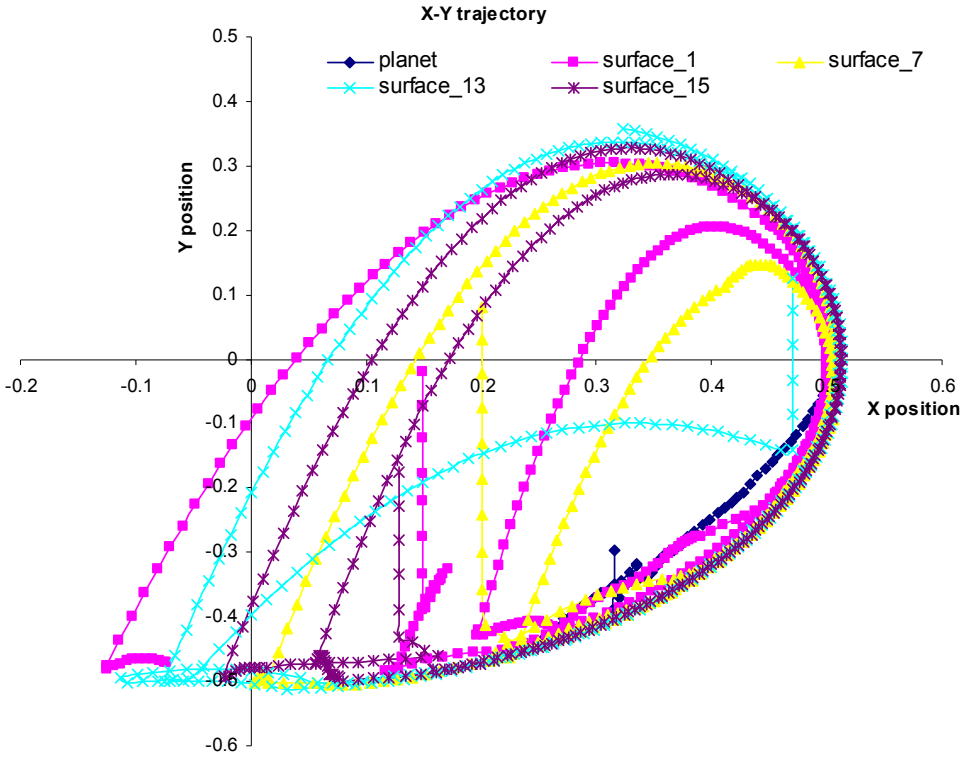

Fig. 10. Particle trajectories for particles of different surface ''roughness''
(mill speed = 2.53 rad/s, 60% of the critical speed)

4.2.2 Collision energy analysis

Figure 11 shows the loss of collision energy for non – spherical particles with respect to tumbling time. Due to a large number of collisions in the beginning of the simulation, higher energies are lost at the initial stage of the tumbling. Once the mill reaches steady-state condition, the rate of energy losses also become uniform and reach a steady-state condition. The less spherical-like surfaces experience a larger number of particle-wall collisions than the more spherical-like particles; as a result, the former loses higher energies in collisions than the latter. This is due to the fact that rougher surfaces have more surface area and contact points than the spherical particles. The mill reaches steady-state after 2.3 s of tumbling time. The initial peaks observed at 0.01 s are simulation artefacts during filling of particles in the mill.

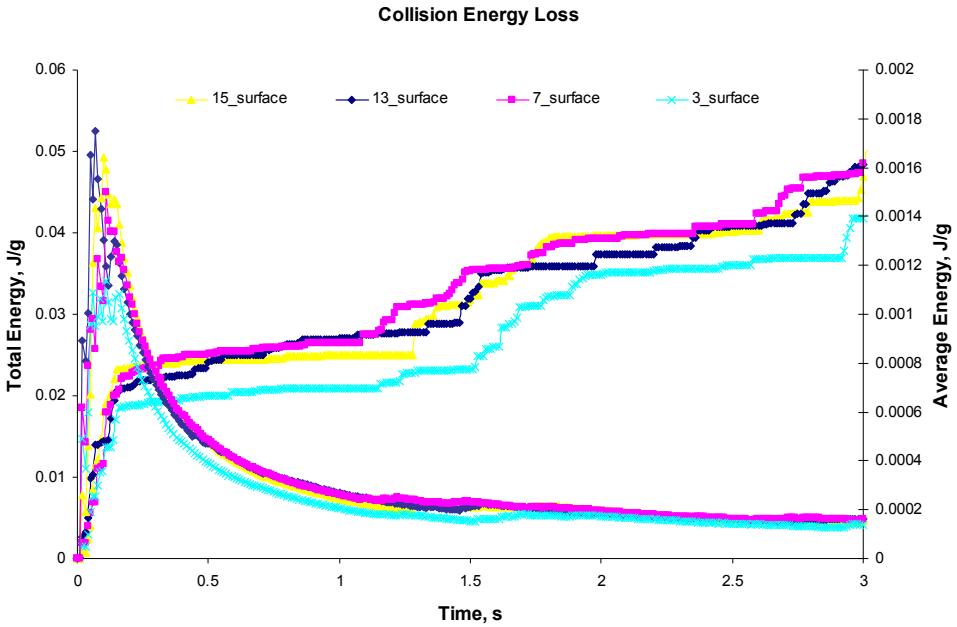

Fig. 11. Total collision energy loss vs. time (mill speed¼2.53 rad=s)

4.2.3 Energy spectra analysis

The frequency distributions of the energy losses can be determined from the individual collision events. These collision energy spectra provide an opportunity to better understand the various contributions to the overall energy dissipation within the mill (Cleary and Morrison, 2004). Knowledge of the effect of mill parameters on the energy spectra will allow selecting useful attributes to increase the efficiency of comminution.

Figure 12 shows the number of collisions with respect to (a) total collision energy loss, (b) normal collision energy loss, and (c) tangential collision energy loss for 3 s of tumbling. Each graph compares the energy losses for different types of particles. The energy spectra distribution in these three graphs shows a similar trend. The maximum energy dissipation is larger for rough particles than smoother particles. The smoother particles experience fewer collisions than the rougher particles, although the total energy dissipation is somewhat similar. A large number of collisions are observed at the lower energies. As noted by Cleary and Morrison (2004), the introduction of additional fines generates more low energy collisions; the rougher particles (having more humps, e.g., 13 surface total, 15 surface total) experience more collisions than the smoother particles at the low energy levels. So, it can be analogized that the rough surfaces or humps are in some way similar to the additional fine particles tumbled in the mill. The input energy per unit mass of particle is an important factor to assess the probability of breakage. Therefore, the humps of the particles may achieve large input energy per unit mass in a collision (sandwiched between particles) with other main particles and are much more likely to be broken because the stress is concentrated in a small zone. Figure 12(b) shows that during collisions, normal energy dissipation is more responsible than the tangential energy dissipation (Figure 12(c)) for abrasion of rougher particles.

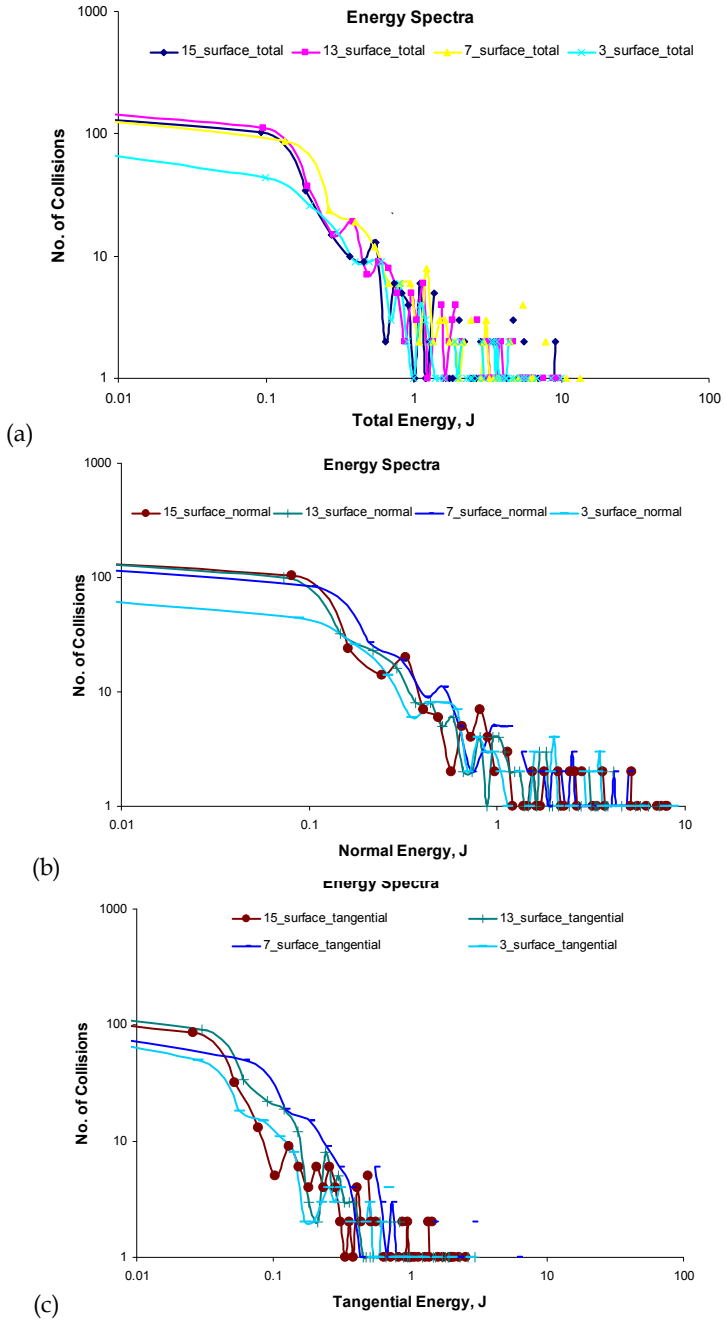

Fig. 12. Number of collisions vs. (a) total energy loss, (b) normal energy loss, and (c) tangential energy loss (mill speed¼2.53 rad=s)

4.3 Testing of hypothesis

Revisiting the hypothesis, the number of collisions increases the mass loss from the parent particles. The experimental mass loss has been compared with the simulated collision energy to test the hypothesis, Figure 13. As mentioned earlier, the tumbling time required to conduct the abrasion test was obtained from the experiments. The abrasion experimental mass loss was compared with the simulated number of collisions, shown in Figure 13.

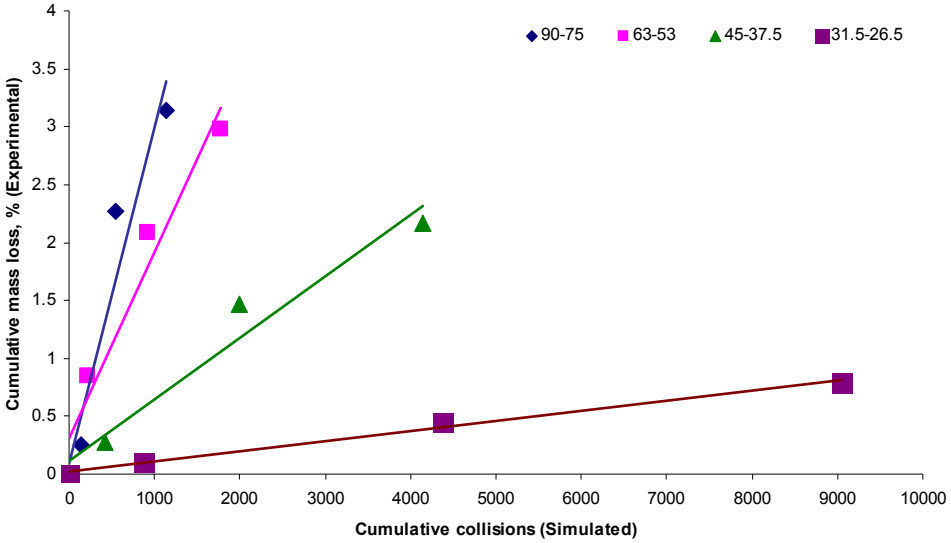

Fig. 13. Experimental mass loss as a function of number of collisions.

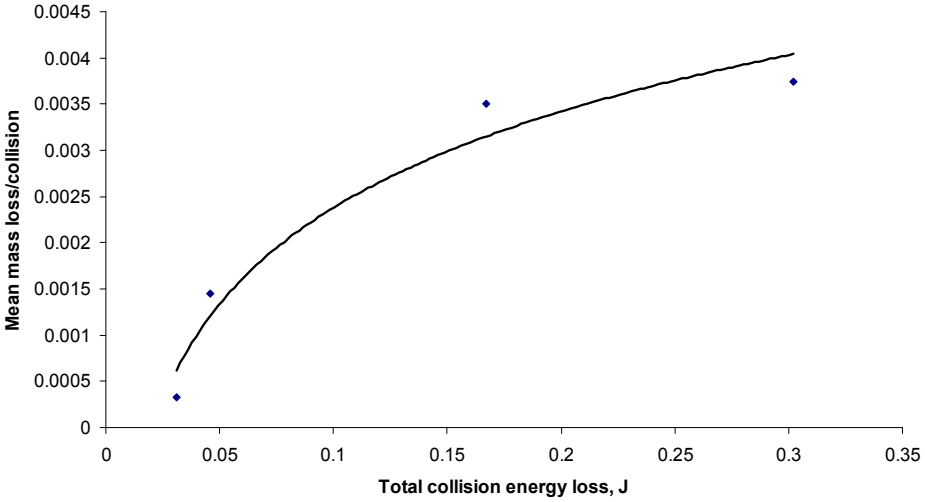

Fig. 14. Mean mass loss per collision (experimental) with respect to the total collision energy estimated from DEM in each size fraction.

The preliminary observations show that as the number of collisions increases, the mass loss from the particles also increases. This indicates that the hypothesis being tested is reasonable. The trend lines in Figure 14 show a very good fit except for 45–37.5 class. Smaller particles lose less mass compared to the larger particles for the same number of collisions. However, due to the limited data points on the graph, it is difficult to relate the nature and degree of dependency of mass loss on the number of collisions for different sized particles.

5. Conclusions

The simulated milling has been carried out in a particle tumbling range (time) which is well below the starting energy required for body breakage of particles. Although the preliminary study shows that the assumed hypothesis (the number of collisions increases the mass loss from the parent particles) is valid, many more experiments have to be carried out to find the nature and degree of dependency of mass loss on abrasion on the number of collisions.

For the less number of particles (considered here for abrasion) the particle–wall collisions are the major cause of particle breakage in the mill as the number of inter-particle collisions are much less compared to the particle–wall collisions. The energy (gain and loss) and energy spectra analysis of particles provided an insight into the dissipation of energies during collision. The force imparted into the particles could be a parameter which depends on the material and the loading process. Hence, further experiments and simulations need to be carried out to study the mechanism of force/energy dissipation during collisions.

The paper also discussed the effect of various abrasion process parameters to investigate their effect in abrasion mechanism of particles. It has been noted that the grinding time affects the comminution of particles. As expected, longer grinding time produces more fragments along with more fines. The size and stiffness of particles also affect the degree of abrasion. For the same mass, smaller particles show more collisions and hence, high degree of abrasion. However, it has been realized that experimental observations are required to validate the effect of size and stiffness of particles in abrasion.

Based on this hypothesis (the number of collisions increases, the mass loss from the particles also increases), it can be concluded that the more irregular particles lose their irregularities (humps and asperities) faster than the more rounded particles. It was observed that as the asperities of the particle decrease, the rate of abrasion decreases. The particle-wall collision is the major cause of particle failure in the mill within the optimum number of particles.

The energy analysis provided insight into the dissipation of energies during collision. During particle-mill shell or particle-particle collision, the asperities of the particles first come in contact with the colliding partner. These asperities will act as stress concentrators on the particles. Based on the energy (gain and loss) and energy spectra analysis of the particles, it was found that the normal collision force is larger than the tangential collision force, and hence the former may be more responsible for the abrasion of particles, i.e., the removal of the asperities of the particles.

6. References

Banini, G.A., 2000. An Integrated Description of Rock Break-age in Comminution Machines, in Julius Kruttschnitt Mineral Research Centre, vol. Ph.D., niversity of Queensland, Brisbane (unpublished).

Cleary, P., Morrison, R., 2004. The Role of Advanced DEM Based Modelling Tools in Increasing Comminution Energy Efficiency. In: Presented at Green processing.

Djordjevic, N., Morrison, R., Loveday, B., Cleary, P., 2006. Modelling comminution patterns within a pilot scale AG/SAG mill. Minerals Engineering 19, 1505– 1516.

EDEM, 2006. DEM Solutions, Edinburgh.

H. Rumpf,Particle Technology, (Translated by F. A. Bull) Chapman and Hall, London (1995).

Khanal, M, Morrison, R, 2008 Discrete element method study of abrasion, Minerals Engineering 21, 751–760

Khanal, M, Schubert, W, Tomas, J 2007, Discrete Element Simulation of bed comminution, Minerals Engineering, Minerals Engineering 20, 179–187

Loveday, B., Morrison, R., Henry, G., Naidoo, U., 2006. An investigation of rock abrasion and break-age in a pilot-scale AG/SAG Mill. In: Presented at SAG 2006, Vancouver, B.C., Canada.

Loveday, B.K., Dong, H., 2000. Optimisation of autogenous grinding. Minerals Engineering 13, pp. 1341–134.

Loveday, B.K., Naidoo, D., 1997. Rock abrasion in autogneous milling. Minerals Engineering 10, 603–612.

Loveday, B.K., Whiten, W.J., 2002. Application of a rock abrasion model to pilotplant and plant data for fully and semi-autogenous grinding. Transaction Institute of Mining and Metallurgy 307, C39–C43.

Morrison, R.D., Cleary, P.W., 2004. Using DEM to model ore break-age within a pilot scale SAG mill. Minerals Engineering 17, 1117–1124.

Solidworks, 2006. Solidworks Inc., SP 4.1 ed.

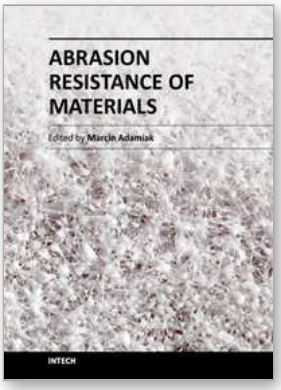

Abrasion Resistance of Materials

Edited by Dr Marcin Adamiak

ISBN 978-953-51-0300-4
Hard cover, 204 pages
Publisher InTech
Published online 16, March, 2012
Published in print edition March, 2012

How to reference

In order to correctly reference this scholarly work, feel free to copy and paste the following:

Manoj Khanal and Rob Morrison (2012). Numerical Simulation of Abrasion of Particles, Abrasion Resistance of Materials, Dr Marcin Adamiak (Ed.), ISBN: 978-953-51-0300-4, InTech, Available from: http://www.intechopen.com/books/abrasion-resistance-of-materials/numerical-simulation-of-abrasion-of-particles-

INTECH
open science | open minds

InTech Europe
University Campus STeP Ri
Slavka Krautzeka 83/A
51000 Rijeka, Croatia
Phone: +385 (51) 770 447
Fax: +385 (51) 686 166
www.intechopen.com

InTech China
Unit 405, Office Block, Hotel Equatorial Shanghai
No.65, Yan An Road (West), Shanghai, 200040, China
中国上海市延安西路65号上海国际贵都大饭店办公楼405单元
Phone: +86-21-62489820
Fax: +86-21-62489821